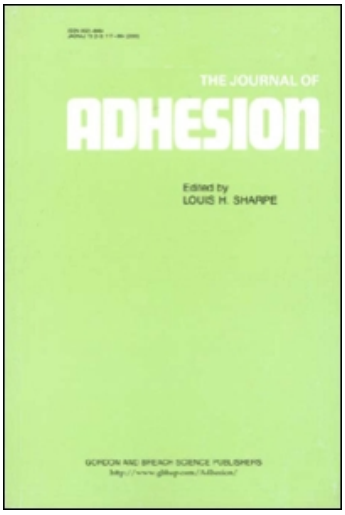

The Journal of Adhesion
Publication details, including instructions for authors and subscription information:
http://www.informaworld.com/smpp/title~content=t713453635

Adhesion Mechanisms of Polyurethanes to Glass Surfaces I. Structure-Property Relationships in Polyurethanes and Their Effects on Adhesion to Glass

Raj K. Agrawal[a]; Lawrence T. Drzal[a]
[a] Department of Chemical Engineering, Composite Materials and Structure Center, Michigan State University, East Lansing, MI, USA

To cite this Article Agrawal, Raj K. and Drzal, Lawrence T.(1995) 'Adhesion Mechanisms of Polyurethanes to Glass Surfaces I. Structure-Property Relationships in Polyurethanes and Their Effects on Adhesion to Glass', The Journal of Adhesion, 54: 1, 79 — 102
To link to this Article: DOI: 10.1080/00218469508014383
URL: http://dx.doi.org/10.1080/00218469508014383

J. Adhesion, 1995, Vol. 54, pp. 79–102
Reprints available directly from the publisher
Photocopying permitted by license only

Adhesion Mechanisms of Polyurethanes to Glass Surfaces I. Structure-Property Relationships in Polyurethanes and Their Effects on Adhesion to Glass*

RAJ K. AGRAWAL and LAWRENCE T. DRZAL**

Department of Chemical Engineering, Composite Materials and Structure Center, Michigan State University, East Lansing, MI 48824, USA

(Received May 25, 1994; in final form August 19, 1994)

Polyurethanes were prepared from toluene diisocyanate (TDI), 1–4-butane diol (BDO) and polycaprolactone-based triols with varying molecular weights. Among each molecular weight triol-based urethane, hard segment content was varied from 20% to 70%. Differential scanning calorimetry, tensile testing, and Iosipescu shear testing were done on all the various urethanes prepared. Thermal characterization data revealed the dependence of phase separation on hard segment content as well as on the triol molecular weight. Tensile data and Iosipescu shear data further confirmed the observations made from the DSC data. The data further indicated that phase separation can greatly improve the modulus of cross-linked segmented urethanes. Adhesion of these urethanes to glass surface was evaluated using soda-lime float glass plate. Urethane samples were cast on the air side of the glass plates and adhesion was measured in shear mode. Adhesion data indicated that in addition to hard segment content, modulus, cross-link density, and molecular weight of the triols, phase separation seems to be a major factor in controlling adhesion. Surfaces of the failed adhesion samples were also analyzed and the failure mode was found to be cohesive, in varying degree, with the different urethane systems.

KEY WORDS Adhesion; polyurethane; glass; phase separation; hard segment content; molecular weight; DSC; Iosipescu shear test; cross link density; modulus.

INTRODUCTION

Reinforced reaction injection molding (RRIM) and structural reaction injection molding (SRIM) of urethanes are widely used in automotive industry to make body panels, fascias, bumper beams, etc. In these applications, good adhesion between the urethane matrix and the reinforcement (usually glass) is shown to be an important factor in determining overall mechanical properties of these composites.[1–4] Another important and emerging application of RIM-urethane is integral molding of gaskets onto glass panels to produce modular window assemblies (*e.g.*, windshields) for automobiles.[5–7] In

* One of a Collection of papers honoring James P. Wightman, who received the 13th Adhesive and Sealant Council Award at the ASC's 1993 Fall Convention in St. Louis, Missouri, USA, in October 1993.

** Corresponding author.

these modular windows, good adhesion between urethane gaskets and glass panels is essential for the structural integrity of these assemblies in the automobiles.

In the above mentioned applications of RIM-urethane polymers, urethane matrix properties vary from one extreme to the other, from being very soft and elastometric in modular window application to very rigid and of high modulus in RRIM and SRIM applications. There are extensive data reported in the literature[8-9] relating final properties of urethanes to various formulation parameters. These parameters control cross-linking density and phase separation in segmented polyurethanes, thus determining final matrix properties. It has been shown[10-13] that phase separation depends on individual segment length, segment length distribution, intra- and interdomain hydrogen bonding, and several other factors. Recent work by Rao and Drzal[14] has shown that, for the same surface chemistry and matrix chemistry, adhesion varies directly with the matrix modulus in glassy cross-linked epoxies. This study is an attempt to extend this relationship to other systems and to correlate the structure-property relationship of segmented polyurethane with its adhesion charcteristics to glass substrates.

Model urethane matrix compositions have been developed that produce a transparent matrix which can be easily prepared and studied in the laboratory. Thermal and mechanical characterization of the matrices have been done to establish matrix properties. Adhesion characteristics of the various matrices to soda-lime float glass plates have been evaluated and correlated with their compositions, structure and properties.

SCOPE OF THE PRESENT WORK

In this study, we have not used any catalyst in the urethane formulations, thus increasing handling time for sample preparation. Also, the polyol used is a triol, allowing us to prepare and study urethanes with a wide range of mechanical properties without having to change their chemistry. Urethane formulations have ranged from those with the lowest possible hard segment content to 100% hard segment content. In this paper, the hard segment content is defined as the percent by weight of the isocyanate and the chain extender in the polymer at fixed stoichiometry or isocyanate index. Thus, in the lowest possible hard segment formulation there is no chain extender, whereas in the 100% hard segment formulation there is no polyol.

To study the role of polyol molecular weight, polyols with three different molecular weights were used to prepare urethane formulations with the same hard segment contents.

EXPERIMENTAL

Materials

The polyurethanes used in this study were caprolactone-based trifunctional polyols available from Union Carbide under the trade name Tone®. Characterstics of these

polyols are listed below:

Polyols	Supplier	Molecular Weight	Hydroxyl Number
Tone 0310	Union Carbide	900	187
Tone 0305	Union Carbide	540	312
Tone 0301	Union Carbide	300	560

Hard segments were made from a 80%–20% mixture of toluene 2,4-diisocyanate and toluene 2, 6-diisocyanate (TDI, Aldrich Chemical Co.), with 1, 4-butanediol (BDO) as a chain extender (Aldrich Chemical Co.).

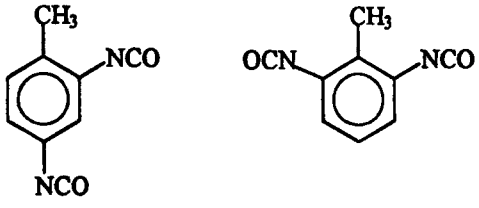

Toluene diisocyanate

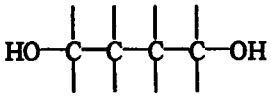

1,4 Butanediol

The various urethane formulations studied in this work are shown in Table I. Their surface free energies, based on contact angle measurements, are between 40.5 and 45.2 Dynes/cm.[15] Also shown in Table I are the weight percent hard segment content and the molecular weight per cross-link (M_c). M_c is the unit weight of the polymer divided by the number of cross-link junctions in the unit weight of the polymer.

The glass substrates used for adhesion testing were annealed 2″ × 5″ × 1/4″ (5.1 × 12.7 × 0.64 cm) soda-lime float glass plaques. Adhesion testing of urethanes was carried out on the air-side of the glass plaques.

Sample Preparation

For Thermal and Mechanical Characterization

A one-step urethane preparation approach was used to prepare all the samples. Triol and BDO chain extender were mixed and degassed for 2–4 hours at 60° C. Silicone rubber molds for casting tensile dogbone specimens and Iosipescu shear specimens

TABLE I
Urethane Formulations at Isocyanate Index of 1.0

Sample Designation	Polyol Type: Tone 0301®	Tone 0305®	Tone 0310®	BDO (Mole%)	TDI (Mole%)	Hard Segment (wt%)	Molecular Weight per Cross-Link (M_c)
10A	—	—	X	0	60	22	1160
10B	—	—	X	22	56	37	1424
10C	—	—	X	31	54	47	1692
10D	—	—	X	34	53	60	2222
10E	—	—	X	41	52	67	2752
5B	—	X	—	7	58	37	854
5C	—	X	—	20	56	47	1013
5D	—	X	—	31	54	59	1324
5E	—	X	—	36	53	67	1646
1C	X	—	—	0	60	47	563
1D	X	—	—	18	57	59	739
1E	X	—	—	26	55	67	912
HS	—	—	—	50	50	100	—

were also subjected to degassing at the same time. Degassing the molds helps in void-free sample preparation by removing the trapped air and moisture in the micro voids present in the molds. The stoichiometric amount of TDI was then added to the triol-chain extender mixture and homogenized with a magnetic stirrer for about a minute. The resultant mixture was then quickly cast into the degassed silicone molds. The filled molds were then heated for 24 hours at 90°C in a convection oven. After curing, samples were taken out of the molds and were sanded and polished to achieve uniform thickness.

For Adhesion Testing

The air side of 2″ × 5″ × 1/4″ (5.1 × 12.7 × 0.64 cm) annealed soda-lime float glass plaques was cleaned with methyl ethyl ketone solvent and dried. Silicone molds with a 1/4″ × 1/4″ × 1/4″ (0.64 × 0.64 × 0.64 cm) cavity were placed on the air side of the glass plaques and were secured to the glass plaques using clamps. The degassed and homogenized mixture of the polyol, the chain extender, and the isocyanate was then poured into the 1/4″ × 1/4″ × 1/4″ (0.64 × 0.64 × 0.64 cm) cavities formed by the glass plaques and silicone molds. The glass plaque-silicone mold assemblies were then cured for 24 hours at 90°C in a convection oven. Upon cooling, the silicone molds were separated from the glass plaques and the samples were stored for adhesion testing. Figure I shows the drawing of an adhesion sample with two urethane blocks cast on a soda-lime glass plate.

Testing and Characterization

Differential Scanning Calorimetry

DSC scans on all the cured urethane samples were done on a Shimadzu TA50 thermal analysis system. Sample weights used for the scans were approximately 20–25 mg. The

DSC cell, with the sample inside the cell, was cooled down to − 80 °C by liquid nitrogen and scans were done at 10°C/min to up to 280°C. No visual sample degradation was observed after the first DSC run. For the second DSC scan on the same sample, the DSC cell was allowed to cool down to ambient temperature in about 12 hours and then liquid nitrogen was used to cool it down further to − 80°C.

Dynamic Mechanical Analysis (DMA)

Rectangular bars (30 mm × 4 mm × 1.25 mm) of various urethane samples were used for dynamic mechanical analysis on a Seiko Instrument DMS-90 system. Values of E′ and tan δ at various temperatures were obtained in clamped three-point bending oscillation mode of deformation at 1 Hz fixed frequency. The temperature was varied from − 70°C to 280°C at 10°C/min.

Iosipescu Shear Testing

All urethane samples for the Iosipescu testing were sanded and polished to a uniform thickness of 2.5 mm. Strain gage rosettes (from Micro Measurements Inc.) were attached to the front of each specimen. Testing was done on a servohydraulic testing machine using a modified Wyoming fixture[16] at 0.05″/minute (0.13 cm/minute) cross-head speed. A strain gage on each sample was connected to a Wheatstone bridge in a half-bridge configuration. The Wheatstone bridge was connected to a signal-conditioning amplifier, and the amplified analog signal was converted to digital signal through a circuit completion box which was connected to a microcomputer-controlled data acquisition system. At least three samples were tested for each urethane formulation. For softer urethane formulations such as 10 A and 10 B, reinforcing tabs were glued to the sample ends to facilitate testing.

Tensile Testing

Dogbone-shaped urethane samples were tested on a tabletop Instron 4201 testing machine using pneumatically-actuated grips. Grips were separated at 2″/minute (5.1 cm/minute) and the stress-strain curve of the sample to failure was recorded on a chart recorder. At least four samples were tested for each urethane formulation.

Adhesion Testing

Adhesion of urethane matrix to glass surface was evaluated using soda-lime float glass plates as the substrate. Plate glass was chosen rather than fibers as the glass-matrix interface/interphase in plate glass could further be analyzed with relative ease using visual, microscopic, spectroscopic, and chemical means.

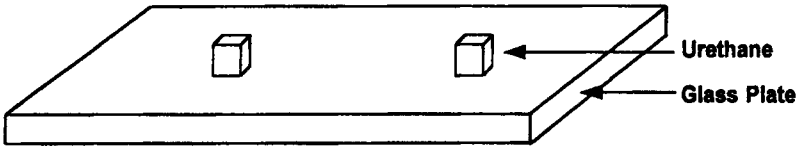

FIGURE 1 Glass–urethane adhesion sample.

The lap-shear configuration for adhesion testing with glass plates could not be used successfully due to the brittleness of the glass plates. In the lap-shear configuration trials, glass plates broke during sample loading or during sample testing due to the slight misalignment or bending. To overcome this, ASTM test method D4501 for measuring shear strength of adhesive bonds between rigid substrates by the block-shear method was modified for this study. Figure 2 shows the front and the rear view of the test fixture with an adhesion sample clamped in place.

An Instron 4201 tabletop testing machine was utilized for the adhesion testing. The test fixture was mounted on the Instron and an adhesion sample was loaded in the test fixture carefully such that the cast urethane block of the sample would engage with the shearing bar of the test fixture. Upon the sample loading, the jaws of the Instron machine were moved apart at 0.2"/minute (0.51 cm/minute). In this fashion, the cast urethane block was shear loaded in a plane parallel to the glass plaque. The maximum load required for the detachment of the urethane block from the glass surface was recorded. At least five samples were tested for each urethane formulation. After failure, glass and urethane samples were saved for failure mode analysis.

Scanning Electron Microscopy (SEM)

Glass surfaces of the failed adhesion samples were examined by SEM. The surfaces were gold coated (approximately 100 Å thickness) by a Denton Vacuum DESK II coater. An ISI-SS130 scanning electron microscope was used to examine the samples. A 50X magnification was utilized in the SEM examination.

X-Ray Photoelectron Spectroscopy (XPS)

Subsequent to adhesion testing, failed glass surfaces were analyzed using Perkin-Elmer PHI5400 x-ray photoelectron spectrometer. An approximately 1/4" × 1/4" (0.61 × 0.61 cm) square area was sectioned from the failed glass surface and was placed inside the XPS chamber. The XPS spectra were obtained at a base pressure of approximately 10^{-9} Torr. The standard Mg K_α source was used for all samples analysis and was operated at 300 W (15 kV, 20 mA). A continuously variable angle sample stage was used and was set to 45° (photoelectron take-off angle). The portion of the sample analyzed by the spectrometer is set through an initial lens system and was set for a 2.0 mm diameter circle. Data were collected in the fixed analyzer transmission mode utilizing a position-sensitive detector and a 180° hemispherical analyzer. Pass energies were set at 89.45 eV for the survey scans (0–1000 eV) and at 35.75 eV for the narrow scans of the elemental regions. Data collection and manipulation was performed with an Apollo 3500 workstation running PHI ESCA software.

RESULTS AND DISCUSSION

Figure 3 shows a simplified two-dimensional schematic representation of possible molecular arrangements in some of the urethane formulations studied in this work.

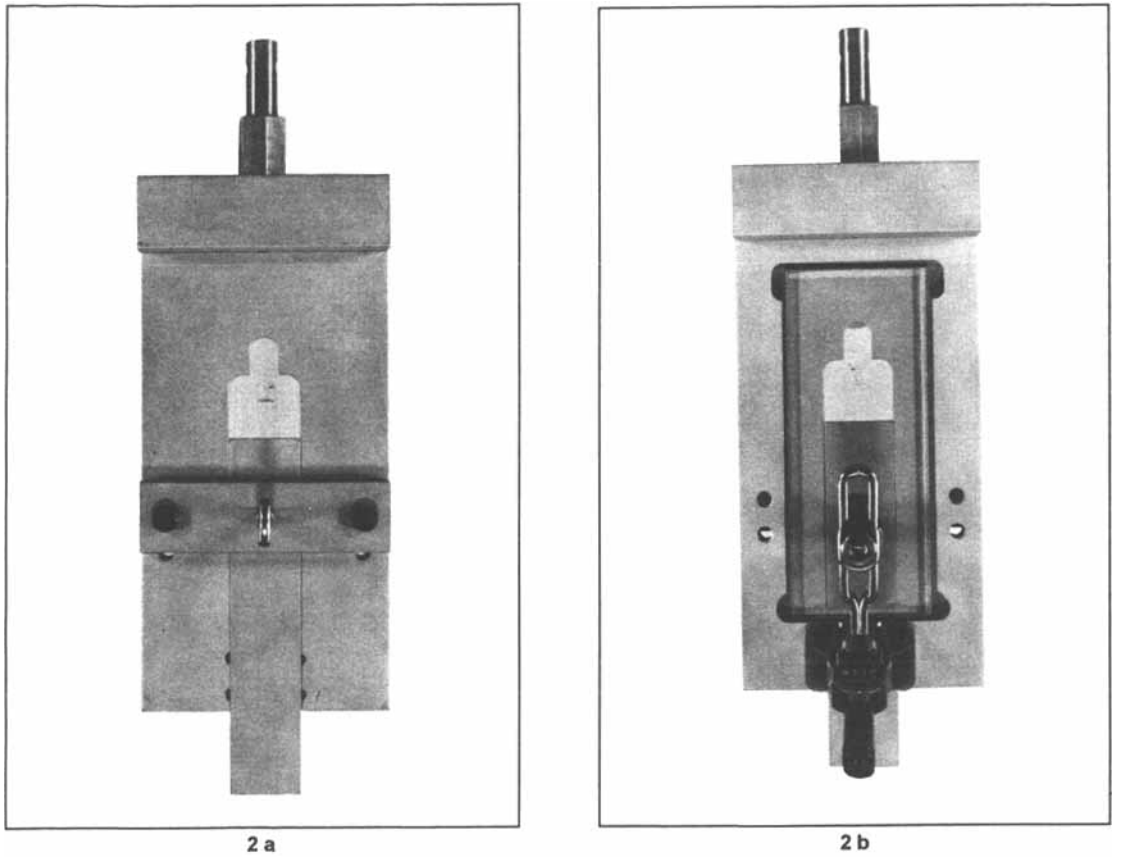

FIGURE 2 Glass-urethane adhesion testing fixture. (a) Front view of fixture with specimen clamped in place. (b) Rear view of fixture with specimen clamped in place.

Figure 3A shows urethane formulation 10A which has no chain extender. From the schematic, it is clear that sample 10A is a cross-linked, single-phase urethane system. Figure 3B, C, and D represent urethane formulations 10E, 5E, and 1E respectively, all with the same hard segment content (~67%). Among these three samples, sample 10E has the highest amount of the chain extender. This can lead to longer hard segment chain lengths resulting in better phase separation.[9-10] In Figure 1D, the soft segment chain length is almost equal to the chain extender and, thus, very little phase separation is expected.

Thermal Characterization

Phase separation phenomena in segmented urethanes can be related to their thermal transition behavior. DSC analysis was used to study thermal transitions in all the synthesized urethane samples. DSC thermograms for urethanes based on Tone 0310 are shown in Figure 4. There can be several thermal transitions in a segmented urethane related to soft segment, hard segment, hydrogen bonding between domains, crystallization, phase melting, etc.[17-19]. In Figure 4, the soft segment transition, which is below 0°C, is difficult to detect consistently and reliably and, thus, is not reported here. The thermal transition above 0°C, which is the most prominent in these scans, can be related to the hard segment. These hard segment thermal transition data are shown in Table II for all the samples based on Tone 0310® (the highest molecular weight triol) based polyurethanes. The glass transition temperature for all the Tone® polyols is approximately − 60°C, whereas for the formulation with 100% hard segment (Sample HS, Table I) is 98.4°C. From Figure 4 it is clear that in the Tone 0310® system, as the hard segment content increases, the transition temperature increases. With higher hard segment content, hard segment chain length increases and longer chain lengths improve phase separation.[9-10] Thus, the increase of thermal transition temperature with increasing hard segment content in the Tone 0310® system suggests that the degree of phase separation improves with hard segment content. Figure 5 shows second DSC thermograms on the same samples after annealing and quenching. The thermal transition temperatures from the second DSC run are, in general, higher than the corresponding thermal transition temperatures from the first DSC run. This suggests that sample annealing and quenching improves phase separation in segmented polyurethanes.[19] The first and second DSC run thermograms of Tone 0305® and Tone 0301® polyol-based urethanes are shown in Figures 6, 7, 8, 9, respectively, and the thermal transition temperature data are shown in Table II. In the first and second DSC runs of the Tone 0305® system, the thermal transition temperature increases with increasing hard segment content. But sample annealing and quenching does not seem to have much effect on the transition temperatures as evidenced by comparing the corresponding first and second DSC transition temperatures. In Tone 0301® based polyurethanes, transition temperature decreases with increasing hard segment content in the first DSC run and remains the same or increases somewhat in the second DSC run. We think the lower transition temperature of the 1E sample in the first DSC run could be the result of extremely short gel time. This may explain why the transition temperature of 1E increases to 106.9°C in the second DSC run from 86.7°C in the first DSC run.

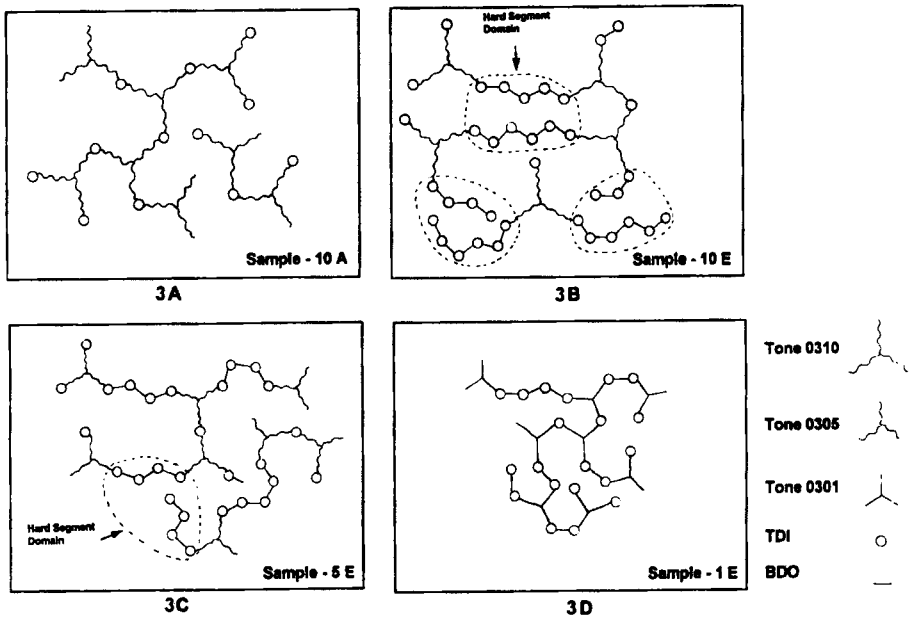

FIGURE 3 Model of molecular arrangements in urethanes.

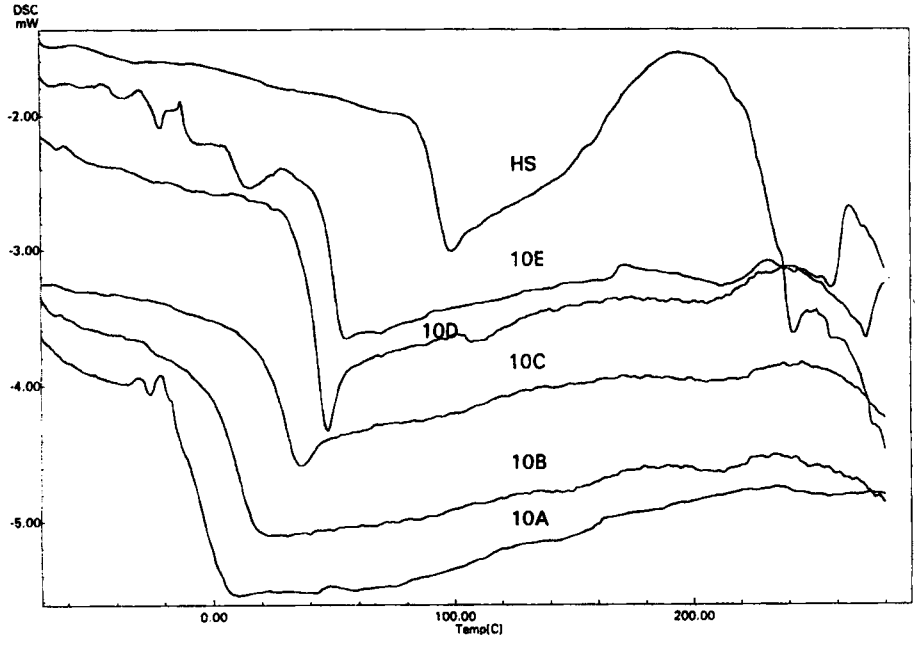

FIGURE 4 DSC thermograms of Tone 0310® based polyurethanes with varying hard segment content (1st Run).

TABLE II
Effects of Hard Segment and Polyol Molecular Weight on Thermal Transitions in Cross-Linked Segmented Polyurethanes

Sample	Polyol Molecular Weight	Hard Segment (wt %)	1st Run Transition Temperature (°C)	2nd Run Transition Temperature (°C)
10A	900	22	6.1	5.3
10B	900	37	19.2	26.5
10C	900	47	35.5	36.3
10D	900	60	46.1	56.7
10E	900	67	54.3	68.2
5B	540	37	44.4	49.4
5C	540	47	59.4	59.9
5D	540	59	64.0	64.8
5E	540	67	73.0	72.2
1C	300	47	100.6	102.2
1D	300	59	98.7	101.3
1E	300	67	86.7	106.9
HS	—	100	98.4	109.8

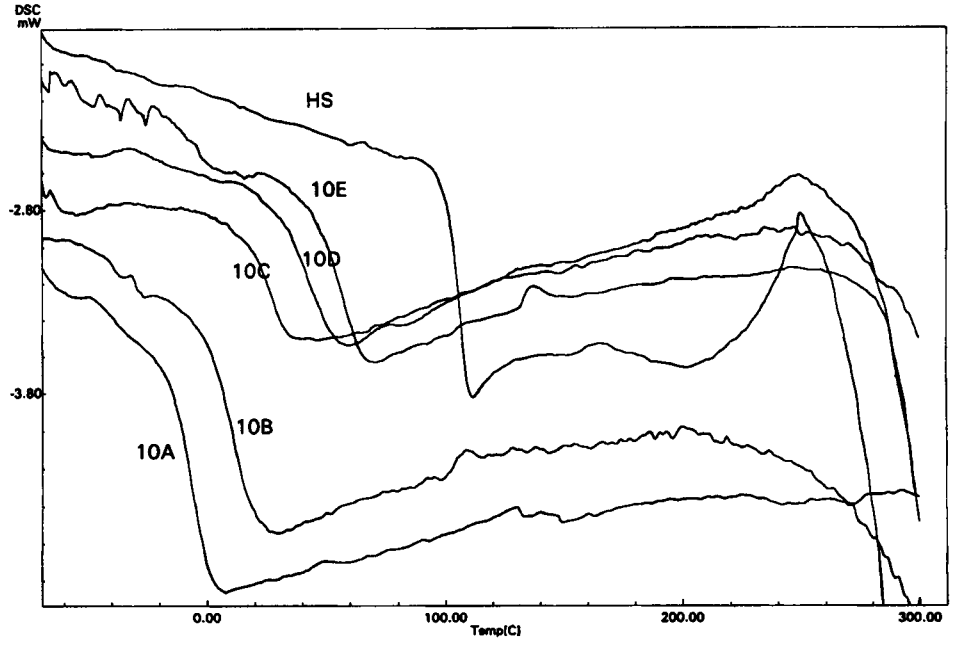

FIGURE 5 DSC thermograms of Tone 0310® based polyurethanes with varying hard segment content (2nd Run).

The DSC transition temperature of Tone 0310®, 0305, and 0301 based polyurethanes from the first run are graphed in Figure 10 and from the second run are graphed in Figure 11 as function of hard gegment content. From both of these graphs it is clear that the rate of increase of transition temperature with the hard segment content

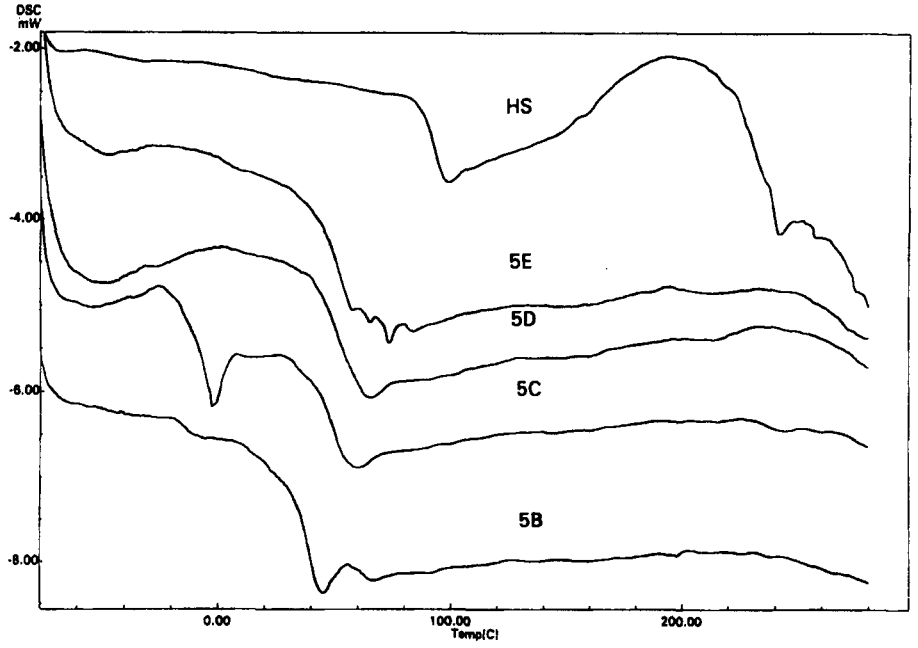

FIGURE 6 DSC thermograms of Tone 0305® based polyurethanes with varying hard segment content (1st Run).

is the highest for Tone 0310® followed by Tone 0305® and Tone 0301®. This suggests that the degree of phase separation increases with hard segment content at a greater rate for higher polyol molecular weight polyurethanes.

These observations are also supported by the dynamic mechanical analysis. Figure 12 shows log (E') *vs.* temperature for samples 1E and 10E which have the same hard segment content. In the figure, we see that the modulus plateau in the rubbery region for the sample 10E is flatter than that for the sample 1E even though the cross-link density in 10E is lower than in 1E. This suggests that the Degree of phase separation in 10E is greater than in 1E.[13]

Mechanical Characterization

All the urethane samples were tested in the tensile mode at 2"/minute (5.1 cm/minute) cross-head separation speed. Load *versus* displacement response of Tone 0310® based polyurethanes is shown in Figure 13 and is found to be highly nonlinear. Samples 10A and 10B showed typical nonlinear and high elongation characteristics of soft, rubbery material. This could be due to strain-induced crystallization in these samples[9,19] even though the samples remained translucent at high strain. Higher hard segment content samples 10C, 10D, 10E and all other samples based on Tone 0305® and Tone 0301® polyols showed yield behavior. Strain at yield for these samples is shown in Table III.

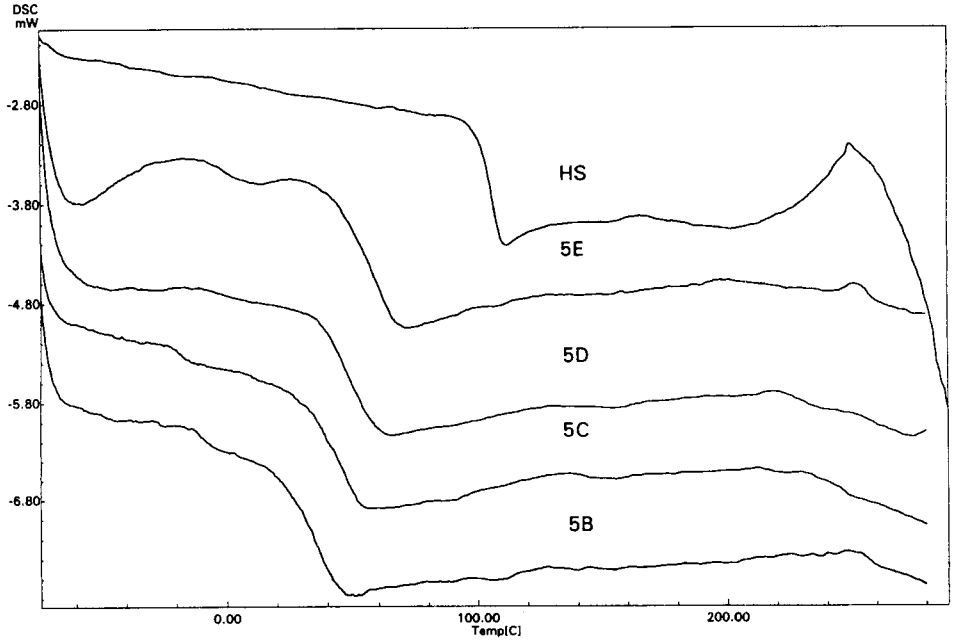

FIGURE 7 DSC thermograms of Tone 0305® based polyurethanes with varying hard segment content (2nd Run).

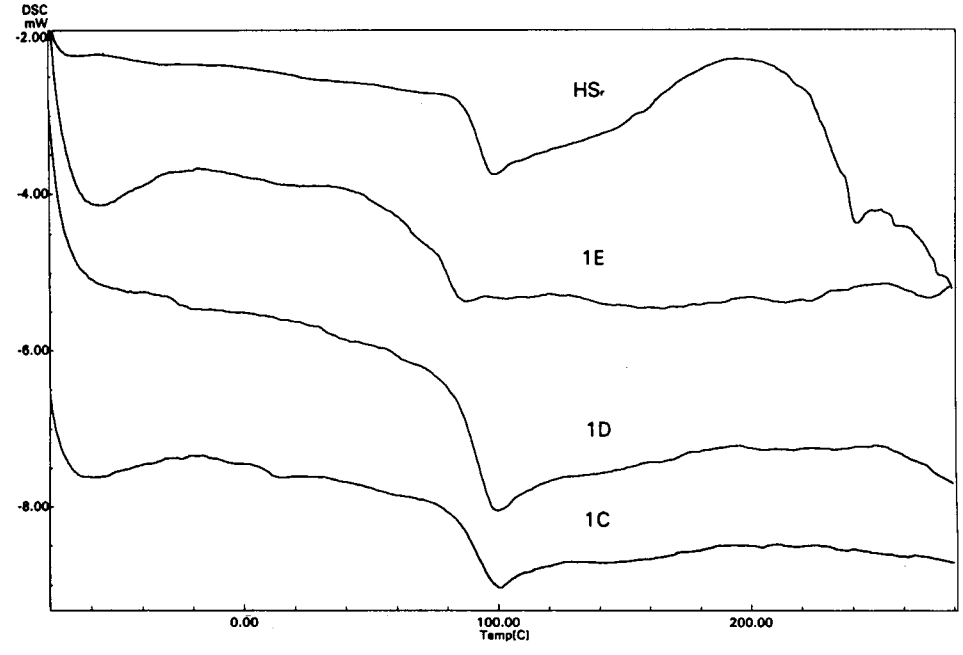

FIGURE 8 DSC thermograms of Tone 0301® based polyurethanes with varying hard segment content (1st Run).

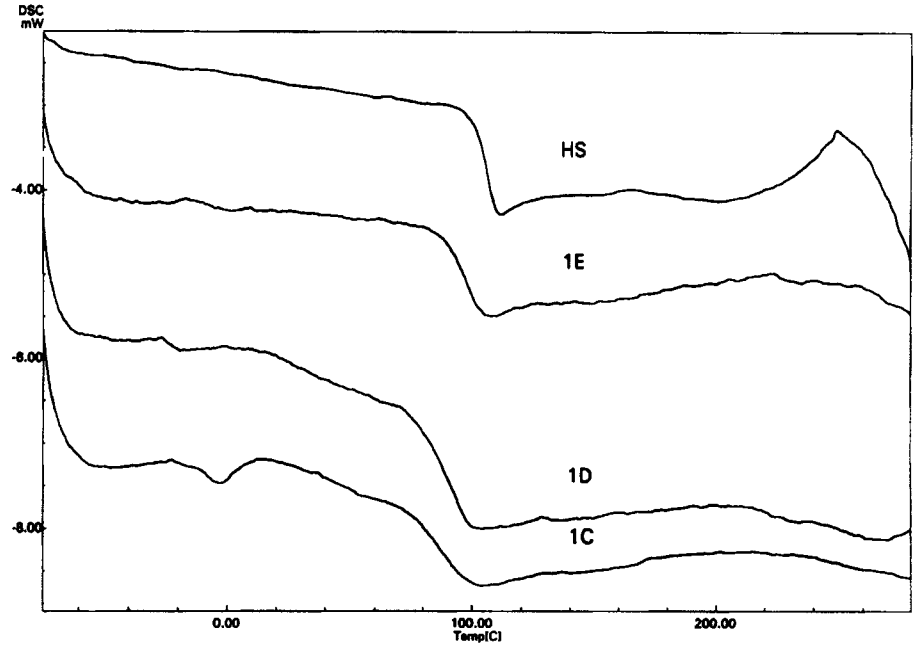

FIGURE 9 DSC thermograms of Tone 0301® based polyurethanes with varying hard segment content (2nd Run).

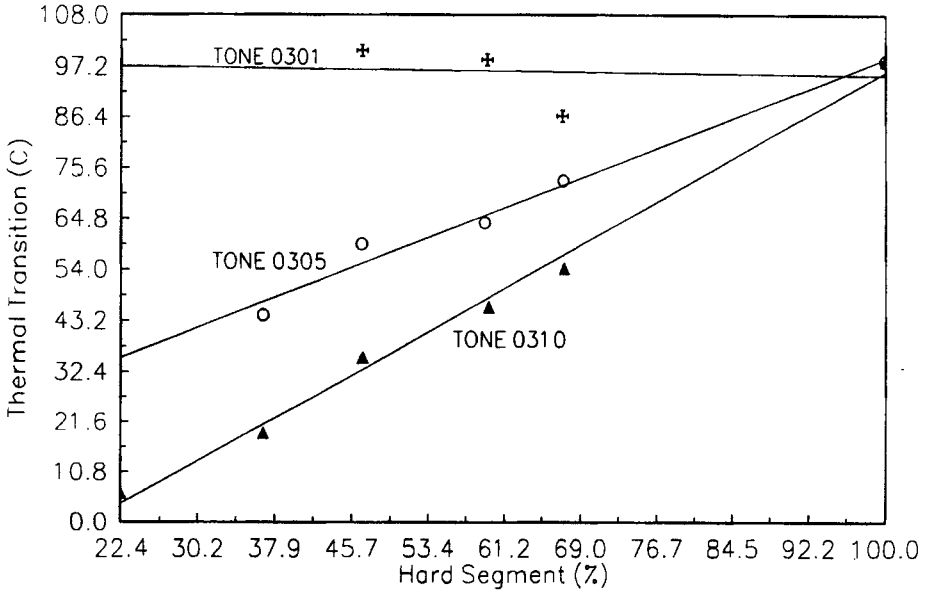

FIGURE 10 Thermal transition temperature *versus* hard segment content in different molecular weight triol-based urethane systems (1st DSC Run).

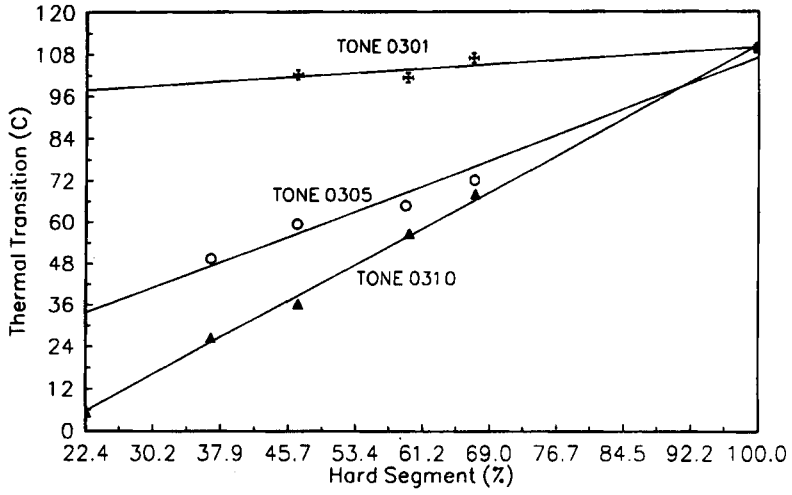

FIGURE 11 Thermal transition temperature *versus* hard segment content in different molecular weight triol-based urethane systems (2nd DSC Run).

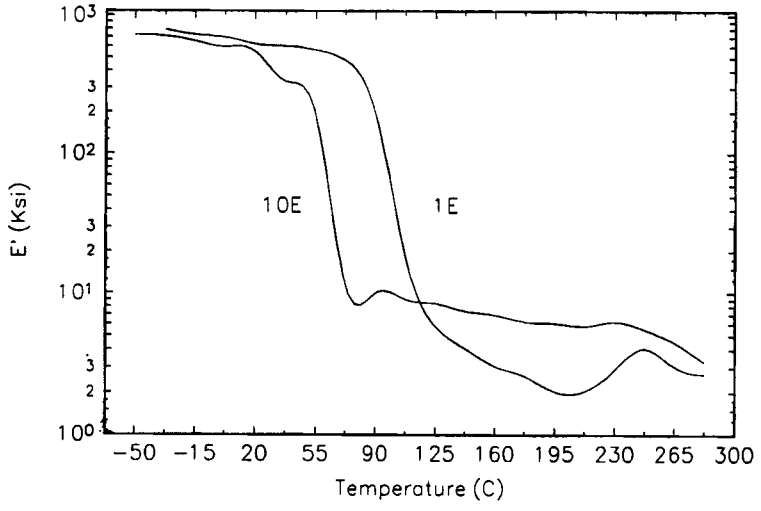

FIGURE 12 DMA scan of Tone 0310® and Tone 0301® polyols based urethanes with constant hard segment content.

Figure 14 shows a semilogarithmic plot of 2% secant tensile modulus *versus* hard segment content of all the urethane samples. The dependence of modulus on hard segment content is nonlinear for Tone 0310® based urethanes whereas it is almost linear on this semilogarithmic plot for Tone 0301® and Tone 0305® based urethanes. The abrupt change in the slope of the Tone 0310® system between sample 10B and 10C suggests that modulus buildup is taking place due to phase separation.[9,13] This further

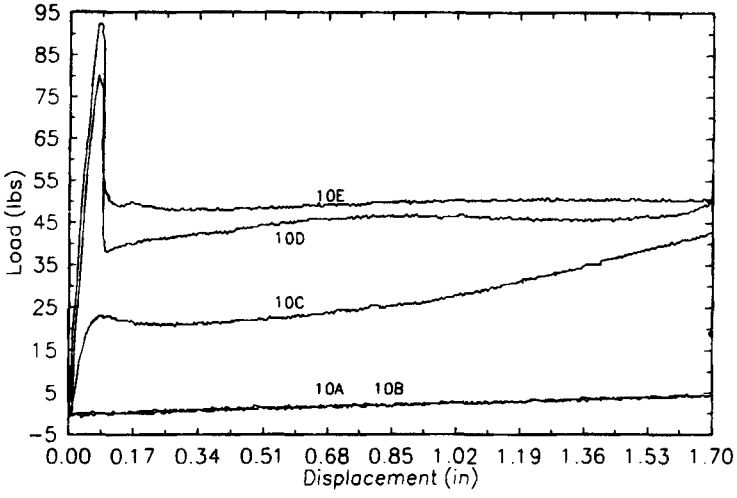

FIGURE 13 Load/displacement response of Tone 0310® based polyurethanes at different hard segment content.

TABLE III
Mechanical Properties of Various Polyurethane Systems

Samples	Shear Modulus (Ksi) 2% Secant	Tensile Modulus (Ksi) 2% Secant	Strain at Yield (%)	Tensile Strength (Ksi)	Hardness (Shore D)
10A	—	0.950	—	0.910	33
10B	—	1.40	—	8.70	50
10C	67.0	103	8.0	6.60	75
10D	151	215	8.2	10.6	80
10E	179	250	8.7	12.3	85
5B	128	116	8.0	8.00	80
5C	150	277	8.0	11.6	84
5D	165	287	8.5	12.6	85
5E	172	306	9.0	13.6	85
1C	176	152	11.0	15.5	87
1D	185	310	11.0	16.5	88
1E	189	349	9.5	15.3	88

supports the observation made earlier from DSC data that higher polyol molecular weight increases the degree of phase separation. Data for tensile strength *vs.* hard segment content for all the urethanes tested are shown in Table III and are graphed in Figure 15. It is clear that, for a given hard segment content, the lower molecular weight polyol systems have higher tensile strengths. This could be due to the higher cross-linking density associated with lower molecular weight triols.

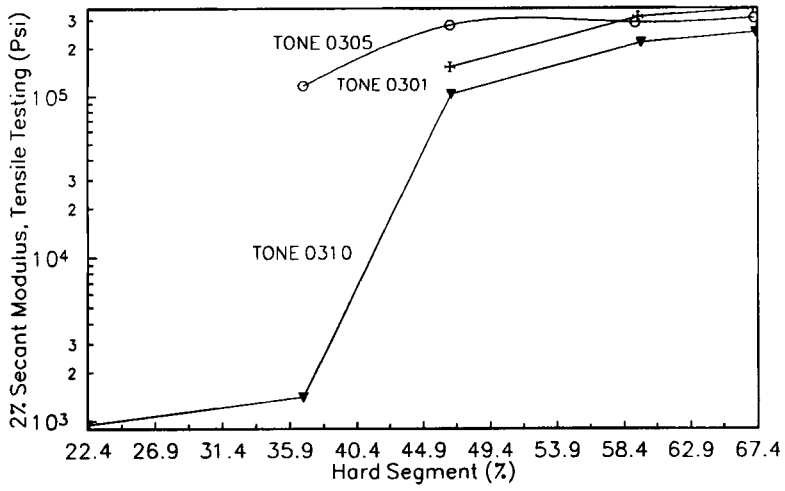

FIGURE 14 2% secant tensile modulus *versus* hard segment content in various urethane systems.

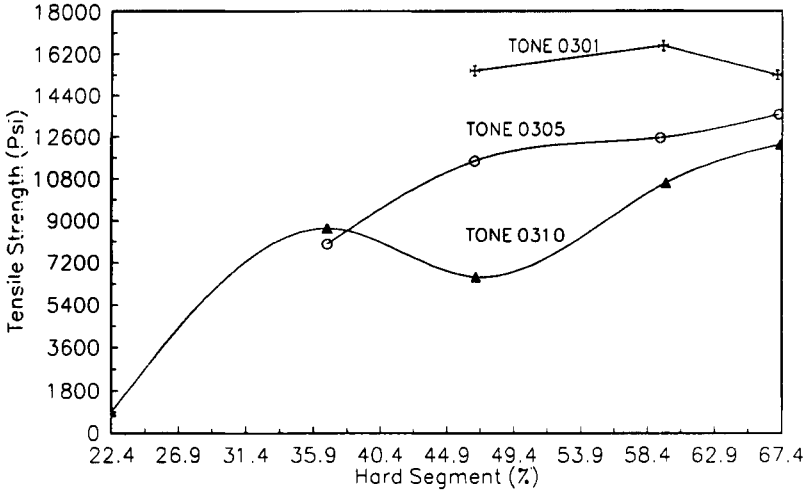

FIGURE 15 Tensile strength *versus* hard segment content in various urethane systems.

Because shear properties of an adhesive or a composite matrix have been shown to be key predictors and scaling parameters, Iosipescu shear testing of all the samples was conducted. Stress-strain data were recorded only up to 8% strain due to the strain gage limitation. Only the shear modulus was determined. Shear strength of most of the samples could not be determined as the samples could not be strained to failure due to limitations of the Iosipescu testing fixture. The samples that did fracture showed a failure pattern characteristic of pure planar shear loading (Figure 16).

Reproducible data for soft, low modulus samples 10A and 10B could not be obtained and are not reported here. Stress-strain response for all the other samples are shown in

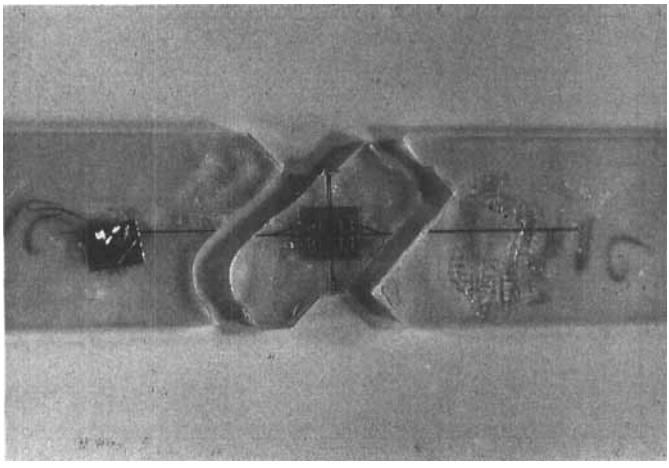

FIGURE 16 Fractured urethane sample after Iosipescu shear testing.

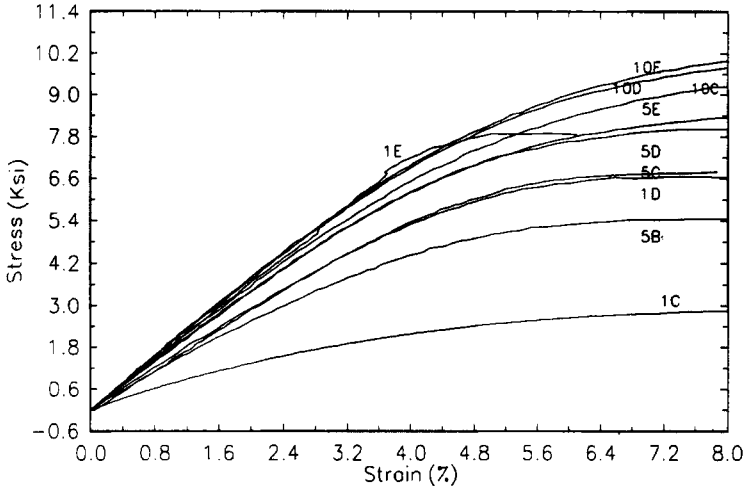

FIGURE 17 Stress/strain response of different urethanes in Iosipescu shear testing.

Figure 17. A 2% secant modulus was calculated and is shown in Table III. Good agreement was found between Iosipescu testing and tensile testing. Figure 18 shows shear modulus *versus* hard segment contents for all the different types of urethanes. From the graph we see that, for the same hard segment content, lower molecular weight polyol-based urethanes have higher moduli. This is due to the higher cross-linking density for the same hard segment content in lower molecular weight triol-based systems. Figure 19 shows the effect of molecular weight per cross-link (M_c) on shear modulus. As M_c increases, cross-link density decreases (see Figure 3) and shear

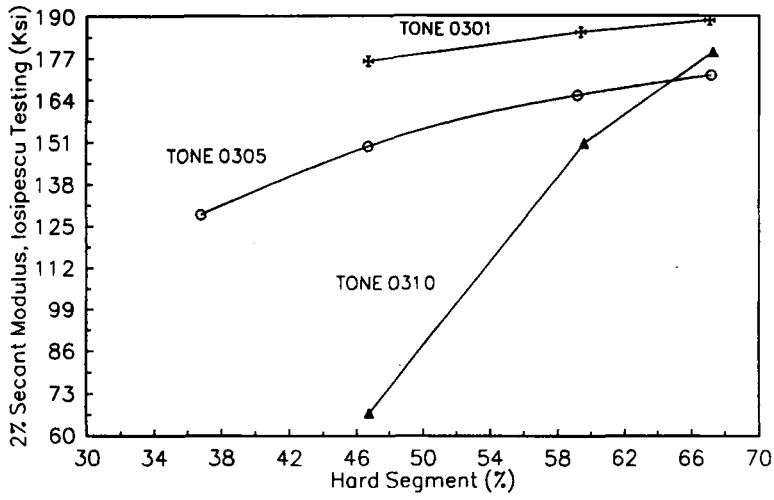

FIGURE 18 2% secant shear modulus *versus* hard segment content in various urethane systems.

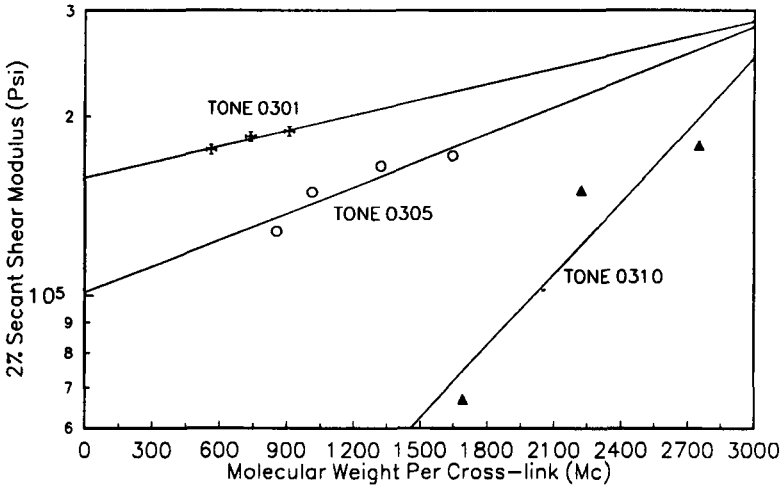

FIGURE 19 2% secant shear modulus *versus* molecular weight per cross-link (M_c) in various urethane systems.

modulus increases. For the same M_c, lower molecular weight polyol systems exhibit higher modulus due to higher hard segment content. Also, in Figure 18, the slope of Tone 0310® based urethane system is higher than that of Tone 0305® and Tone 0301® systems. This is consistent with the tensile testing and suggests that higher molecular weight polyol undergoes phase separation more readily.

TABLE IV
Adhesion of Various Polyurethanes to Glass Surface

Sample	Shear Adhesion (PSi)
10A	706 ± 4
10B	1590 ± 30
10C	2690 ± 60
10D	4640 ± 80
10E	5370 ± 300
5B	4160 ± 110
5C	4280 ± 90
5D	5240 ± 220
5E	5080 ± 360
1C	825 ± 340
1D	2120 ± 530
1E	3020 ± 1360

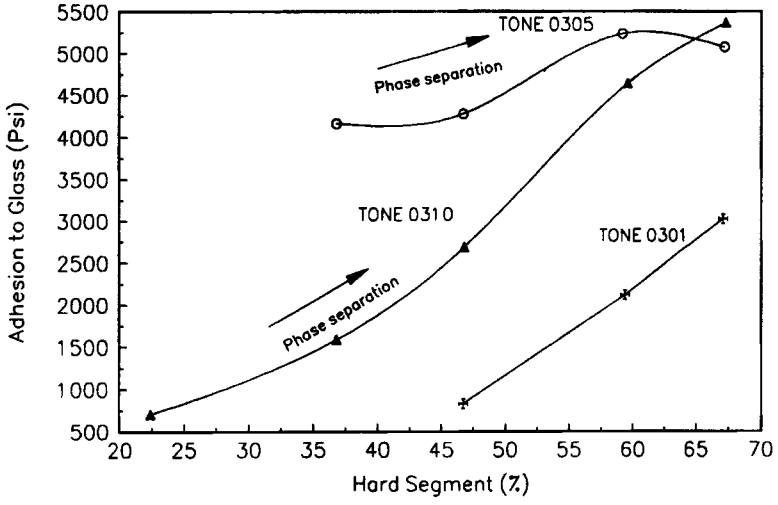

FIGURE 20 Adhesion to glass *versus* hard segment content in various urethane systems.

Adhesion to Glass

Adhesion samples were tested in the shear fixture and the peak load values recorded are shown in Table IV. Samples with Tone 0310® and Tone 0305® showed very good reproducibility, whereas Tone 0301® based samples had a larger variation, especially for sample 1E. Thus, a large number of 1E samples were tested to obtain a reliable mean and standard deviation.

Figure 20 shows adhesion values to glass *versus* hard segment content for all of the three types of urethane systems. Within each family of urethane systems, adhesion

values increase with increasing hard segment content. For the same hard segment content (for example, 10C, 5C and 1C or 10D, 5D, and 1D) Tone 0305® based urethane shows better adhesion than Tone 0310® and Tone 0310® based urethane shows better adhesion than Tone 0301® based urethane.

Rao *et al.*[14,20] have shown that adhesion of graphite fibers to epoxy resin is dependent on the shear modulus of the matrix. A similar plot is made between the shear modulus of the various urethanes and their respective adhesion values to glass in Figure 21. From this figure we see that adhesion does increase with modulus in all the urethane systems and different urethane systems show different dependencies. Higher modulus urethanes based on Tone 0301® show poor adhesion to glass. From the least square fit lines, we see that same level of adhesion could be obtained from the lower modulus sample based on Tone 0310® polyol. Tone 0310® polyol has the highest molecular weight among all the polyols studied and based on thermal and mechanical characterization of these urethanes, we have seen that higher molecular weight polyol enhances phase separation. This suggests that, along with modulus and hard segment content, phase separation in a segmented urethane system can have significant effect on its adhesion to glass.

After adhesion testing, the glass surfaces of the samples were observed for failure mode. Some of the samples had chunks of urethane left on the glass surface while other samples showed brittle failure and did not leave any visibly noticeable urethane. SEM micrographs of Tone 0310® based urethane samples are shown in Figure 22. As was also seen under the optical microscope, SEM confirms the adhesive failure mode in samples 10A, 10B, and 10C and cohesive failure mode in samples 10D and 10E. The circular patterns in micrographs of 10D and 10E could be due to the microvoids present in the sample. To analyze failure modes further, x-ray photoelectron spectroscopy was used for all the samples. A control sample of glass was also run to obtain

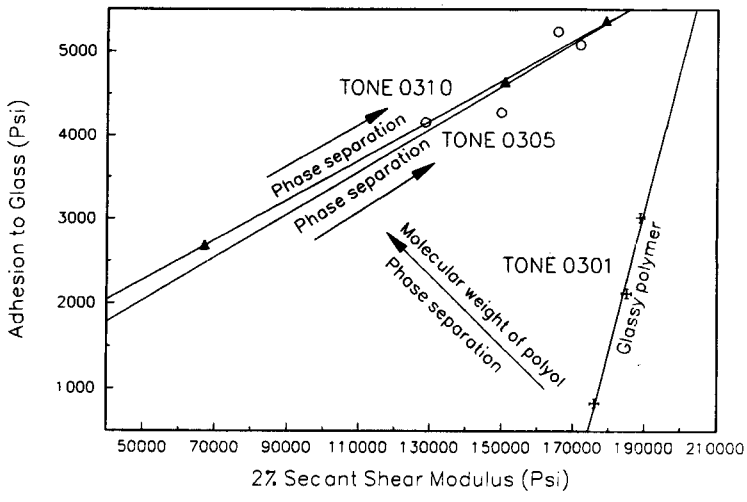

FIGURE 21 Adhesion to glass *versus* shear modulus of various urethane systems.

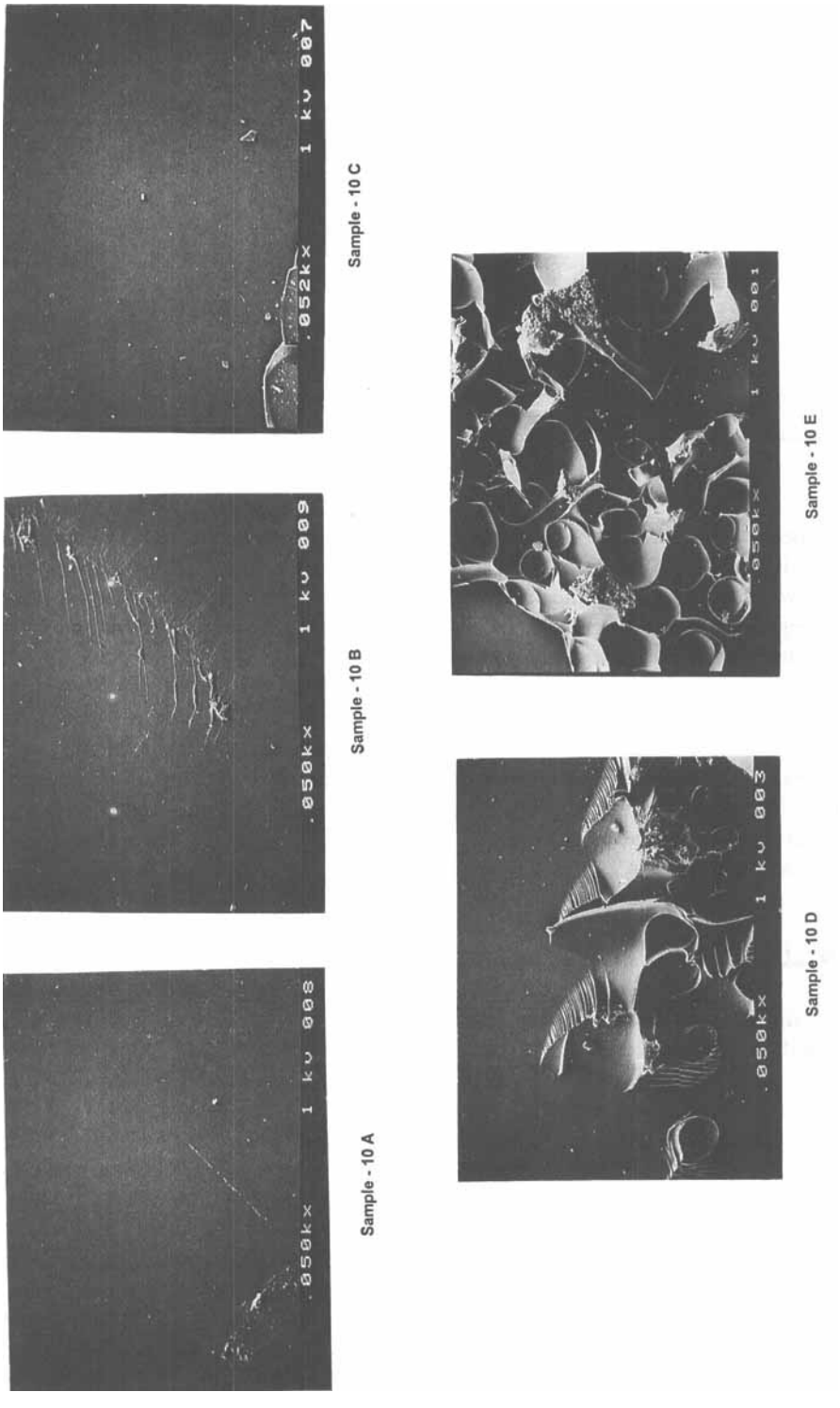

FIGURE 22 SEM micrographs of glass surfaces after adhesion testing of Tone 0310® based polyurethanes.

TABLE V
Atomic Concentration Ratio on Failed Glass Surface from X-ray Photoelectron Spectroscopy

Samples	N/100C	Theoretical Value
10A	2.8	6.8
10B	3.5	9.0
10C	5.9	10.4
10D	6.2	12.2
10E	9.0	13.3
5B	3.7	10.1
5C	6.2	11.4
5D	8.6	12.9
5E	7.8	13.9
1C	4.2	13.0
1D	5.7	14.1
1E	8.1	14.7
Glass	0.8	

baseline data. The presence of nitrogen on the surface was then used as the indicator of residual urethane. Surface atomic concentration ratios of nitrogen per 100 carbon atoms was calculated from the narrow scans of the elemental regions for all the samples and they are shown in Table V. The control sample has an $N/100C$ atomic ratio of 0.84. All of the urethane samples showed higher $N/100C$ ratios than the control glass. This suggests that all of the samples had some degree of cohesive failure in the urethanes. Table V also shows theoretically calculated values of $N/100C$ for all the urethane samples. These values are higher than the experimental values obtained from the glass surfaces. Hearn *et al.*[21] have reported that air cured urethane surfaces in segmented polyurethanes tend to be richer in soft segments. This observation would help explain why surface concentration of nitrogen at the interface could be lower than the bulk nitrogen concentration.

CONCLUSIONS

Three different urethane systems were prepared from caprolactone-based triols with different molecular weights, the same chain extender and the same diisocyanate. Among each urethane system, hard segment content was varied by adding different amounts of the chain extender and the isocyanate. This type of experimental design allowed us to study the effects of hard segment and triol molecular weight on thermal, mechanical, and adhesion characteristics of cross-linked segmented polyurethanes.

DSC results showed that the transition temperature related to the hard segment increased with increasing hard segment content. This could be due to the increased hard segment chain length at higher hard segment content, promoting phase separation in the urethanes. Thus, in a urethane system, phase separation phenomena are favored by increasing hard segment content. Also, the rate of increase of thermal transition temperature in different molecular weight triol-based urethanes indicated that phase separation phenomena were also favored by the higher triol molecular weight.

Both tensile and Iosipescu testing of the urethane samples showed nonlinear stress-strain behavior. The tensile and shear modulus data indicated that with increasing hard segment content within a urethane system, as cross-linking density decreases, the urethane modulus increases. This could be due to several factors, including increased amount of aromatic isocyanate content, increased hydrogen bonding, increased phase separation, and other factors. The modulus of the same hard segment content urethanes was found to be higher for lower molecular weight triols. Thus, cross-linking density seems to be the determining factor for modulus in the constant hard segment content urethanes. In the case of higher molecular weight triol-based urethanes, the amount of increase of modulus with hard segment content is higher than that for the lower molecular weight triol-based polyurethanes. This indicates that phase separation is favored by larger polyol molecules.

Adhesion to glass for these cross-linked polyurethanes seems to be a coupled phenomenon controlled by several factors, including hard segment content, modulus, molecular weight of triols, cross-linking density, and phase separation. In urethanes based on the same molecular weight triols, higher modulus and higher hard segment content increases adhesion to glass. However, equal levels of adhesion can be attained with urethanes having different moduli. Higher molecular weight polyol-based urethanes having lower modulus and lower hard segment content attained adhesion levels equal to urethanes made with lower molecular weight polyols having higher modulus and higher hard segment content. This suggests that, among many other factors, phase separation in cross-linked segmented urethanes can be a key factor in controlling adhesion to glass surfaces.

Acknowledgement

The authors wish to thank the Donnelly Corporation for supporting this work.

References

1. J. R. Dawson and J. B. Shortall, "The Impact Behaviour of RRIM Polyurethane Elastomers," *Cellular Polymers*, **1**, 41–51 (1982).
2. C. Kau, A. Hiltner, E. Bear and L. Huber, "Damage Processes in Reinforced Reaction Injection Molded Polyurethanes," *J. Reinforced Plastics and Composite*, **8**, 18–39 (1989).
3. P. C. Yang and W. M. Lee, "Fracture Mechanism Study of Flake Glass Filled RIM Urethane Systems," *J. Elastomers and Plastics*, **19**, 120–146 (1987).
4. E. G. Schwarz, F. E. Critchfield, L. P. Tackett and P. M. Tarin, "Silane Effects and Machine Processing in Reinforced High Modulus RIM Urethane Composites," *J. Elastomers and Plastics*, **11**, 280–300 (1979).
5. A. F. Reilly and J. L. Sanok, "Method and Apparatus for Making Molded Window Gasket," U.S. Patent **4**, 755, 339 (1988).
6. J. K. Fielder and R. Carswell, "Polyurethane RIM Systems for Automotive Modular Windows," *SAE Int. Cong. and Exp.*, Detroit, MI, Paper 900515 (1990).
7. R. K. Agrawal, A. Agrawal and J. Thomas, "Developments in Modular Windows for Automotive Applications," *SAE Int. Cong. and Exp.*, Detroit, MI, Paper 910759 (1991).
8. J. H. Saunders and K. C. Frisch, Polyurethanes, Chemistry and Technology, John Wiley & Sons, Inc., NewYork, NY (1983).
9. C. W. Macosko, "RIM Fundamentals of Reaction Injection Molding" (Hanser Publishers, New York, NY (1989).
10. R. J. Zdrahala, R. M. Gerkin, S. L. Hager and F. E. Critchfield, "Polyether-Based Thermoplastic Polyurethanes. I. Effect of the Hard-segment Content," *J. Appl. Poly. Sci.* **24**, 2041–2050 (1979).

11. Z. S. Chen, W. P. Yang and C. W. Macosko, "Polyurea Synthesis and Properties as a Function of Hard Segment Content," *Rubber Chem. Tech.* **61**, 86–99 (1987).
12. A. L. Chang, R. M. Briber, E. L. Thomas, R. J. Zdrahala and F. E. Critchfield. "Morphology Study of the Structure Developed During the Polymerization of a Series of Segmented Polyurethanes," *Polym.*, **23**, 1060–1065 (1982).
13. R. E. Camargo, C. W. Macosko, M. Tirrell and S. T. Wellinghoff, "Phase Separation Studies in RIM Polyurethanes Catalyst and Hard Segment Crystallinity Effects," *Polym.* **26**, 1145–1154 (1985).
14. V. Rao and L. T. Drzal, "The Dependence of Interfacial Shear Strength on Matrix and Interphase properties," *Polym. Compos.* **12**, 48–56 (1991).
15. Details of Surface Free Energy Measurements will be published in part II of this work in *J. Adhesion Science and Technology* (1994).
16. H. Ho, M. Tasi, J. Morton and G. L. Farley, "An Experimental Procedure for the Iosipescu Composite Specimen Tested in the Modified Wyoming Fixture,"*J. Composites Technol. and Res.*, **15**, 52–58 (1993).
17. C. A. Byrne, J. L. Mead and C. R. Desper, "Structure-property Relationships of Aliphatic Polyurethane Elastomers Prepared from CHDI,"*Advances in Urethane Science and Tech.*, **11** (Technomic Publications, LanCaster, PA, 1992), pp. 68–109.
18. W. P. Chen, K. C. Frisch and S. W. Wong, "The Effect of Soft Segment on the Morphology of Polyurethane Elastomers," *Advances in Urethane Science and Tech.*, **11** Technomic Publications, (1992), pp. 110–136.
19. C. Hepburn, *Polyurethane Elastomers* Lancaster, PA, (Elsevier Science Publs., New York, NY, 1992).
20. V. Rao and L. T. Drzal, "The Temperature Dependence of Interfacial Shear Strength for Various Polymeric Matrices Reinforced with Carbon Fibers," *J. Adhesion* **37**, 83–95 (1992).
21. M. J. Hearn, B. D. Ratner and D. Briggs, "SIMS and XPS Studies of Polyurethane Surfaces 1. Preliminary Studies," *Macromolecules* **21**, 2950–2959 (1988).